

Gene expression patterns and related pathways in the hearts of rhesus monkeys subjected to prolonged myocardial ischemia

Xiaojuan Liu^{1,2}, Jingyao Zhang^{1,3}, Pengfei Li^{1,4}, Pengfei Han¹, Y James Kang¹ and Wenjing Zhang⁵ 

¹Regenerative Medicine Research Center, Sichuan University West China Hospital, Chengdu 610041, China; ²Institute of Medical Biology, Chinese Academy of Medical Sciences and Peking Union Medical College, Kunming 650118, China; ³Core Facilities of West China Hospital, Sichuan University, Chengdu 610041, China; ⁴Key Laboratory of Molecular Pathology, Inner Mongolia Medical University, Hohhot 010059, China; ⁵Department of Genetics, Genomics and Informatics, College of Medicine, University of Tennessee Health Science Center, Memphis, TN 38163, USA

Corresponding authors: Wenjing Zhang. Email: wzhang67@uthsc.edu; Y James Kang. Email: ykang7@uthsc.edu

Impact Statement

Pathological ventricular remodeling in the late stage of myocardial infarction is associated with the appearance of heart failure. The imbalance in the expression remarkably changed genes, including natriuretic peptide A/B and *corin*, and its related pathways may play an important role in aggravating cardiac remodeling. The novel revealed molecular mechanisms found in the monkey model provide some molecular pathways that can be considered during the exploration of diagnostic reagents and therapeutic targets in the late phase of myocardial infarction.

Abstract

After myocardial infarction (MI) occurs, progressive pathological cardiac remodeling results in heart dysfunction and even heart failure during the following months or years. The present study explored the molecular mechanisms underlying the late phase of MI at the global transcript level. A rhesus monkey model of myocardial ischemia induced by left anterior descending (LAD) artery ligation was established, and the heart tissue was collected eight weeks after ligation for transcriptome analysis by DNA microarray technology. Differentially expressed genes in the core infarcted area and remote infarcted area of the ischemic heart were detected with significance analysis of microarray (SAM), and related pathways were detected by Gene Ontology (GO)/pathway analysis. We found that compared to the sham condition, prolonged ischemia increased the levels of 941 transcripts, decreased the levels of 380 transcripts in the core infarcted area, and decreased the levels of 8 transcripts in the remote area in monkey heart tissue. Loss of coordination between the expression of genes, including natriuretic peptide A (*NPPA*), *NPPB*, and *corin*

(*Corin*, serine peptidase), may aggravate cardiac remodeling. Furthermore, imbalance in the enriched significantly changed pathways, including fibrosis-related pathways, cardioprotective pathways, and the cardiac systolic pathway, likely also plays a key role in regulating the development of heart remodeling.

Keywords: Myocardial infarction, prolonged ischemia, DNA microarray technology, gene expression, pathways, rhesus monkey

Experimental Biology and Medicine 2023; 248: 350–360. DOI: 10.1177/15353702231151968

Introduction

Ischemic heart disease (IHD) is usually caused by an imbalance in the myocardial supply and demand of blood. Diabetes mellitus, hypertension, hyperlipidemia, obesity, old age, cigarette smoking, and atherosclerosis are the main risk factors for IHD. IHD can lead to myocardial infarction (MI) or ischemic stroke,¹ and has become one of the top three causes of death globally, causing approximately 7.2 million deaths each year; it has a high incidence, mortality, and disability.² Due to the loss of contractile tissue, the ventricular tissue is remodeled in both infarcted area (IA) and non-IA to adapt to the stimulation within a few hours after MI occurs, and the remodeling continues to progress.^{3,4} Ventricular remodeling

after MI is also associated with functional changes in the infarcted heart, including a progressive increase in the end-systolic volume index, a decline in the ejection fraction, and even heart failure.^{5,6}

Several pathways and genes are involved in the regulation of pathological cardiac remodeling after MI. In the early stage of MI, inflammatory and immune signaling pathways, metabolic pathways and myocardial contraction pathways change markedly until 24 h post-MI.^{7,8} In the late phase of MI, the main features of cardiac remodeling, including ventricular wall thinning, myocyte hypertrophy,⁹ and myocardial fibrosis,¹⁰ lead to heart failure. Several molecular mechanisms have been revealed in our previous studies on a rhesus monkey model of MI induced by left anterior

descending (LAD) artery ligation surgery. We found that suppression of the expression of angiogenic factors is associated with reduced capillary density,^{11,12} and increased lysyl oxidase (LOX) activity enhances collagen deposition in the ischemic area,¹³ all of which may aggravate the dysfunction of the heart.

However, the current knowledge about the mechanisms in the late phase of MI is still fragmented. In view of this, we explored the molecular mechanisms involved in the pathological process of prolonged ischemia in the heart by identifying alterations in gene expression and related pathways at the global transcript level. The availability of DNA microarray technology provides an opportunity to study the changed gene profile in any given tissue or cell.¹⁴ A myocardial ischemia model in rhesus monkeys established by LAD artery ligation surgery was used to mimic human pathophysiology.

Materials and methods

Animals and animal care

Male rhesus monkeys (*Macaca mulatta*), aged 2–3 years and weighing 4.5–6.0 kg, were obtained from the Chengdu Ping-An experimental animal breeding and research center, a non-human primate center in Sichuan Province accredited by the Chinese government. The monkeys were acclimated to the laboratory conditions in the Association for Assessment and Accreditation of Laboratory Animal Care-accredited facility for a period of at least one month. The animal diet, feeding conditions, environment enrichment, and amelioration of the pain after surgery followed the descriptions in our previous studies.^{12,13} The animal care and experimental procedures were all approved by the Institutional Animal Care and Use Committee at Sichuan University West China Hospital following the guidelines of the US National Institutes of Health.

MI monkey model

The experimental procedures were described in our published studies.^{12,13} Briefly, monkeys were divided into two groups: the sham-operated control (sham, $n = 3$) and MI ($n = 3$) groups. The monkeys in the MI group were intubated after anesthesia, and their hearts were exposed via the left fourth intercostal thoracotomy incision (4–5 cm) in the chest wall. Then, MI was induced by the permanent ligation of the LAD artery after three rounds of ischemia reperfusion for the LAD artery, which were conducted by a 1-min occlusion followed by a 5-min reperfusion. The operation of the sham group was consistent with that of the MI group except for the ligation of the LAD artery.

Tissue preparation

The monkeys were sacrificed by intravenous injection of potassium chloride at eight weeks after the surgery. Specific involved heart areas of the monkeys in the MI group were obtained: the IA, which was distinguished from the normal tissue through its pale appearance and stiffness, and the remote area (RA), which was the area at least 3 mm away from the IA. The two parts of the heart from the MI group and the heart tissue from the sham group were all collected

in RNAlater® RNA Stabilization Solution (Invitrogen, USA) for total RNA extraction.

DNA microarray

Total RNA from MI or sham-operated hearts was extracted using TRIzol® Reagent (Invitrogen, USA) and quantified by a spectrophotometer. The integrity of the total RNA was detected by agarose gel electrophoresis. The DNA microarray technology and part associated bioinformatics analysis were supported by CapitalBio Corporation Company, Beijing, China. The experimental procedures provided by the company were followed. Briefly, an initial amount of 100 ng of total RNA from the heart tissue was used, and the following procedures, including the first round of synthesis of first-strand cDNA and second-strand cDNA, the synthesis of cRNA, the purification of the cRNA by nucleic acid binding beads, the second round of synthesis of first-strand cDNA, the hydrolysis of the cRNA, and the purification of the single-stranded DNA, were performed sequentially according to the experimental procedures of an Ambion® WT Expression Kit (Affymetrix, USA). The single-stranded DNA was quantified by a spectrophotometer and then fragmented by a WT Terminal Labeling Kit (Affymetrix, USA). After detecting the distribution range of the cDNA fragment size, which needed to be distributed between 40 and 70 nt, by gel-shift analysis (Invitrogen, USA), a WT Terminal Labeling Kit was used to place biotin labels on the fragmented single-stranded DNA, and the labeling efficiency was detected by gel-shift analysis.

The cDNA was hybridized to a Rhesus Gene 1.1 ST Array Plate (Affymetrix, USA) and stained by using a Hybridization, Wash, and Stain Kit (Affymetrix, USA). The probe array was scanned by a GeneChip® Scanner 3000 Scanner (Affymetrix, USA) controlled by the Affymetrix® GeneChip® Command Console® Software (AGCC).

Bioinformatics analysis

The .DAT files presented in the image signal obtained from the scanner were transformed into .CEL files presented in the digital signal by AGCC. The .CEL files were used as source files to perform data preprocessing via Log Scale Robust Multiarray (RMA) analysis,¹⁵ including background correction, integration of the probe signal into the probe group (probe set) signal, and signal normalization to remove the variability between samples from different groups caused by non-biological factors. Among 26,353 enriched probes detected by DNA microarray technology, approximately 81.53% probes were eliminated, as they showed either ineffective signal values or undefined gene symbols after normalization. The *Macaca* database in DAVID (<https://david.ncifcrf.gov/home.jsp>) was used to annotate the genes.

The differentially expressed genes in the IA with sham, RA with sham, and IA with RA comparison were detected by significance analysis of microarray (SAM). Genes with a Q value ≤ 0.05 accompanied by a fold change (FC) (the ratio of IA to sham, RA to sham or IA to RA) ≥ 2 or ≤ 0.5 were defined as significantly upregulated (FC ≥ 2) or downregulated (FC ≤ 0.5) genes. The up- or downregulated genes are shown in scatter plots.

Cluster analysis was used to test the relevance of the gene expression patterns by Cluster 3.0 Manual software. The data used in the cluster analysis were derived from the normalized gene signal value and analyzed by hierarchical and average linkage methods.

To investigate the pathways and functions related to the differentially expressed genes to reveal the molecular mechanisms involved in the pathological process of MI, pathway analysis based on the Kyoto Encyclopedia of Genes and Genomes (KEGG) database and Gene Ontology (GO) analysis probing the functional gene function in three categories (cellular component, molecular function, and biological process) were performed with Molecular Annotation System (MAS) 3.0.

Real-time quantitative reverse-transcription polymerase chain reaction

The protocols for total mRNA extraction, reverse transcription, real-time polymerase chain reaction (PCR) and data analysis were followed as described in our previous study.¹² The primers were as follows: *NPPB*, 5'-CCAAGATGGTGCAAGGGTCT-3' (forward) and 5'-TAATGCCGCTCAGCACTTT-3' (reverse); *TBP*, 5'-TGCTCACCCACCAACAGTTT-3' (forward); and 5'-TGCTCTGACTTTAGCACCTGT-3' (reverse).

Statistical analysis

The data are shown as the mean \pm SD. Unpaired *t*-tests and hypergeometric distribution algorithms were used in the present study. At least three independent experiments were carried out. A *Q* value \leq 0.05 combined with an FC \geq 2 or FC \leq 0.5 was considered to indicate significance in the SAM assay, and significant changes judged by a *P* value $<$ 0.05 were used in the pathway and GO analyses.

Results

Alteration of the gene expression pattern in the heart after prolonged myocardial ischemia

The heart tissues used in the present study were from the same monkey models as in our previous report, and the infarcted myocardia were verified by hematoxylin and eosin (H&E), Sirius red, and Masson's trichrome staining.¹²

In total, 4680, 5174, and 4756 gene expression signal values were obtained in the sham, IA, and non-IA (remote area, RA) groups, respectively, after normalization. Among the screened differentially expressed genes, prolonged myocardial ischemia increased the signals of 941 probes and decreased the signals of 380 probes in the IA group compared with the sham group, but only 8 changed probe signals were enriched in the RA group, and all probes were downregulated. As expected, the signals of 843 probes were increased and the signals of 406 probes were decreased in the IA group compared with the RA group. The increased, decreased, and unchanged probe signals in the IA with sham, RA with sham, and IA with RA comparisons are shown as volcano plots in Figure 1(A) to (C).

The overall view of the gene expression patterns in the heatmap in Figure 1(D) shows that the repeatability of the experiments in every group was good, as the three parallel

samples were all clustered. In addition, the cluster of the IA group, in which approximately two of three genes were upregulated, was distinguished from the clusters of the sham group and the RA group, with few differences observed between the sham and RA groups. These findings indicated that the gene expression patterns were changed remarkably in the IA due to prolonged myocardial ischemia but that prolonged ischemia had little effect on the non-IA under the same conditions.

Upregulated genes in the ischemic heart after prolonged ischemia

The top 10 upregulated genes, adjusted by *Q* values and sorted by FC values, in the IA with sham and IA with RA comparisons are shown in Table 1. No genes were upregulated in the RA group compared with the sham group. The most significantly upregulated gene in the IA group compared with the sham group in the late phase of MI was natriuretic peptide A (*NPPA*), which plays a key role in cardio-renal homeostasis through regulation of natriuresis, diuresis, and vasodilation. Another natriuretic peptide family member, natriuretic peptide B (*NPPB*), which also contributes to cardio-renal homeostasis, was also upregulated by 15.5666-fold in the IA group. In addition, the upregulated genes in the IA, including thrombospondin 4 (*THBS4*) and nephroblastoma overexpressed gene (*NOV*), also contribute to cardioprotection after stimulation. Genes that regulate cell motility, growth, or differentiation were dramatically upregulated in the IA group compared with the sham group, including versican (*VCAN*); extracellular growth factor (EGF)-containing fibulin-like extracellular matrix protein 1-like (*EFEMP1*); secreted frizzled-related protein 4 (*SFRP4*); SPARC-related modular calcium-binding protein 2-like (*SMOC1*); and collagen, type III, alpha 1 (*COL3A1*). In addition, when the IA group was compared with the RA group, the gene expressions of *NPPA*, *NOV*, *VCAN*, *EFEMP1*, and *SMOC1* were also upregulated in the IA group, with lower FC values than those in the comparison of the IA group with the sham group. Prolonged ischemia also specifically upregulated the gene expression of ceruloplasmin (*CP*), thrombospondin 2 (*THBS2*), tenascin C (*TNC*), and adipocyte enhancer-binding protein 1-like (*AEBP1*) in the IA group compared to the RA group.

Quantitative reverse-transcription polymerase chain reaction (RT-qPCR) analysis of *NPPB* mRNA expression was performed to confirm the microarray data (Figure 1(E)).

Downregulated genes in the ischemic heart after prolonged ischemia

Among the top 10 downregulated genes in the comparison of the IA group with the sham group (Table 2), *corin* (Corin, serine peptidase) was the most remarkably downregulated gene. Corin is a serine protease in the heart and cleaves pro-*NPPA* or pro-*NPPB* to the active form to prevent dilated cardiomyopathy from progressing into heart failure by promoting salt and water excretion.^{16,17} The functions/components of the other top 10 downregulated genes in the comparison of the IA group with the sham group were as follows: DNA replication (including NAD-dependent DNA ligase, *ligA*), oxidoreductase activity (including dehydrogenase/reductase

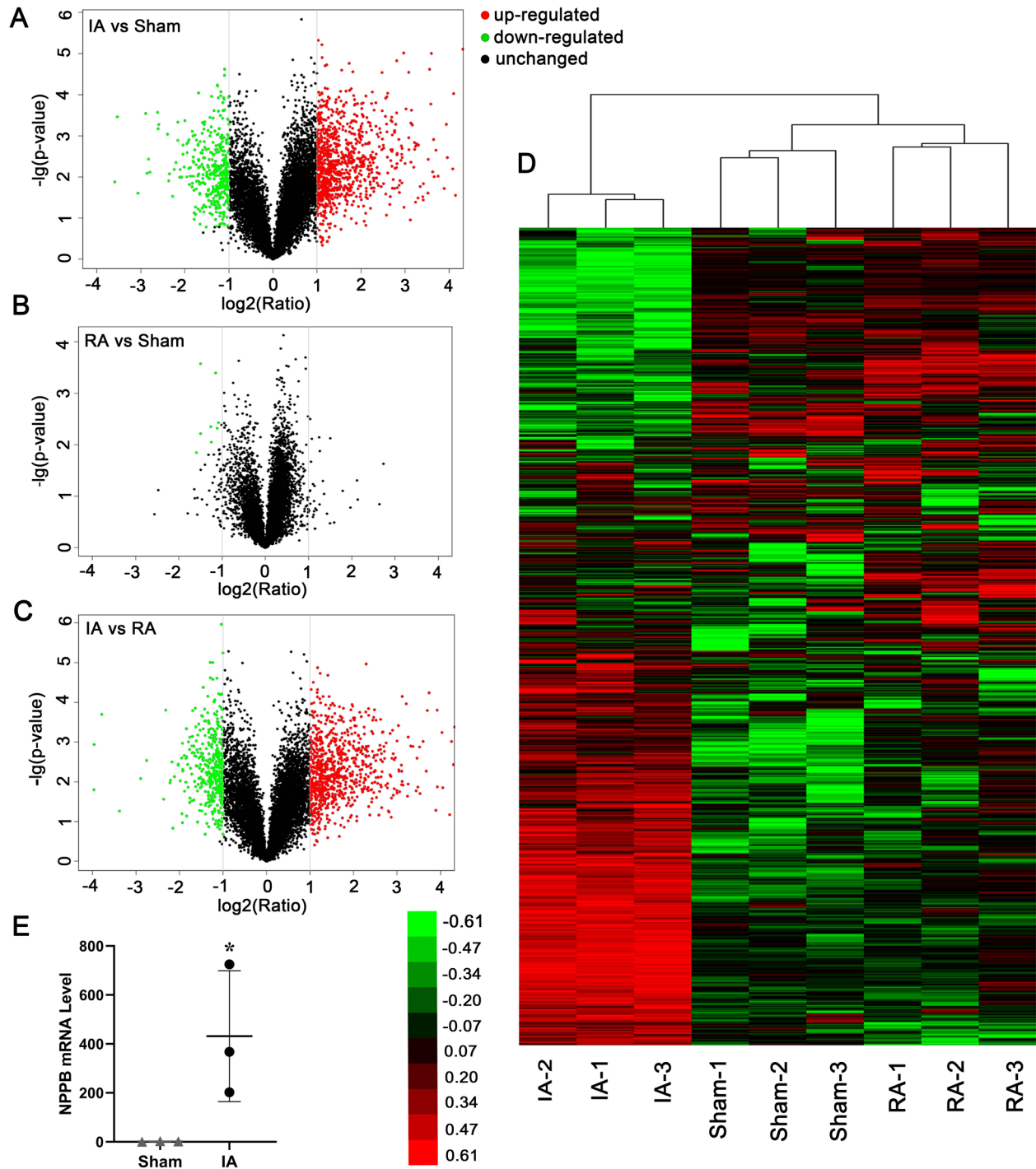


Figure 1. Gene expression patterns in monkey heart tissue. Volcano plots showing the significantly changed genes in the comparisons of (A) the infarcted area (IA) group with the sham group, (B) the remote area (RA) group with the sham group, or (C) the IA group with the RA group by significance analysis of microarray (SAM). Each point represents a gene expression signal. A Q value ≤ 0.05 and fold change (FC) ≥ 2 or ≤ 0.5 were considered to indicate a significant change. (D) Hierarchical cluster analysis of gene expression patterns in the sham, IA, and RA groups. Each rectangle represents a gene expression signal. (E) RT-qPCR analysis of the mRNA expression of *NPPB*. * $P \leq 0.05$ versus sham group. (A–D) Upregulated genes are colored red, downregulated genes are colored green, and genes without changes are colored black.

SDR family member 7C-like, *DHRS7C*, and flavin containing monooxygenase 2, *FMO2*), nervous system development (including nuclear receptor subfamily 4 group A member 2, *NR4A2*, and fibroblast growth factor 12, *FGF12*), fibrous sheath (including amyotrophic lateral sclerosis 2 chromosome region candidate 12, *ALS2CR12*), inhibition of metalloproteinases (including TIMP metalloproteinase inhibitor 4, *TIMP4*),

apoptosis resistance (including phosphatidylethanolamine-binding protein 4, *PEBP4*), and bactericidal activity (including defensin beta 1, *DEFB1*). *DEFB115*, another member of the *DEFB* family, was also downregulated in the RA group compared to the sham group (Table 2). When the IA group was compared with the RA group, a tendency was observed in the gene expressions of *corin*, *DHRS7C*, *DEFB1*, *FGF12*, and

Table 1. Top 10 upregulated genes in hearts subjected to chronic myocardial ischemia.

ID	Gene name	Functions	FC
IA vs sham			
1	Natriuretic peptide A (<i>NPPA</i>)	Hormone that plays a key role in mediating cardio-renal homeostasis, and is involved in vascular remodeling and regulating energy metabolism.	39.5601
2	Versican (<i>VCAN</i>)	May play a role in intercellular signaling and in connecting cells with the extracellular matrix. May take part in the regulation of cell motility, growth, and differentiation. Binds hyaluronic acid.	33.8225
3	EGF-containing fibulin-like extracellular matrix protein 1-like (<i>EFEMP1</i>)	Binds EGFR, the EGF receptor, inducing EGFR autophosphorylation and the activation of downstream signaling pathways.	33.4518
4	Thrombospondin 4 (<i>THBS4</i>)	Adhesive glycoprotein that mediates cell-to-cell and cell-to-matrix interactions and is involved in various processes, including cellular proliferation, migration, adhesion and attachment, inflammatory response to CNS injury, regulation of vascular inflammation, and adaptive responses of the heart to pressure overload and in myocardial function and remodeling.	32.0951
5	Complement C1q tumor necrosis factor-related protein 3-like (<i>CTRP3</i>)	<i>CTRP3</i> is an adipokine with pleiotropic functions in cell proliferation, glucose and lipid metabolism, and inflammation.	27.0516
6	Nephroblastoma over-expressed gene (<i>NOV</i>)	Regulation of cell apoptosis, tumor invasion, and tumor metastasis.	24.2085
7	Latent-transforming growth factor beta-binding protein 2-like (<i>LTBP1</i>)	Key regulator of transforming growth factor beta (TGFB1, TGFB2, and TGFB3) that controls TGF-beta activation by maintaining it in a latent state during storage in extracellular space.	23.0516
8	Secreted frizzled-related protein 4 (<i>SFRP4</i>)	Function as modulators of Wnt signaling through direct interaction with Wnts. They have a role in regulating cell growth and differentiation in specific cell types (by similarity).	21.3911
9	SPARC-related modular calcium-binding protein 2-like (<i>SMOC1</i>)	Plays essential roles in both eye and limb development. Probable regulator of osteoblast differentiation.	19.8608
10	Collagen, type III, alpha 1 (<i>COL3A1</i>)	Collagen type III occurs in most soft connective tissues along with type I collagen. Involved in regulation of cortical development.	17.6959
IA vs RA			
1	Versican (<i>VCAN</i>)	May play a role in intercellular signaling and in connecting cells with the extracellular matrix. May take part in the regulation of cell motility, growth, and differentiation. Binds hyaluronic acid.	27.4615
2	EGF-containing fibulin-like extracellular matrix protein 1 (<i>EFEMP1</i>)	Binds EGFR, the EGF receptor, inducing EGFR autophosphorylation and the activation of downstream signaling pathways.	20.2731
3	Nephroblastoma over-expressed (<i>NOV</i>)	Regulation of cell apoptosis, tumor invasion, and tumor metastasis.	19.0714
4	Natriuretic peptide A (<i>NPPA</i>)	Hormone that plays a key role in mediating cardio-renal homeostasis, and is involved in vascular remodeling and regulating energy metabolism.	16.5886
5	SPARC-related modular calcium-binding protein 2-like (<i>SMOC1</i>)	Plays essential roles in both eye and limb development. Probable regulator of osteoblast differentiation.	16.3932
6	Latent-transforming growth factor beta-binding protein 2-like (<i>LTBP1</i>)	Key regulator of transforming growth factor beta (TGFB1, TGFB2, and TGFB3) that controls TGF-beta activation by maintaining it in a latent state during storage in extracellular space.	15.2188
7	Ceruloplasmin (ferroxidase) (<i>CP</i>)	Ceruloplasmin is a blue, copper-binding (6–7 atoms per molecule) glycoprotein. It has ferroxidase activity oxidizing Fe(2+) to Fe(3+) without releasing radical oxygen species. It is involved in iron transport across the cell membrane.	13.3460
8	Thrombospondin 2 (<i>THBS2</i>)	Adhesive glycoprotein that mediates cell-to-cell and cell-to-matrix interactions. Ligand for CD36 mediating antiangiogenic properties.	12.9640
9	Tenascin C (<i>TNC</i>)	Extracellular matrix protein implicated in guidance of migrating neurons as well as axons during development, synaptic plasticity as well as neuronal regeneration. Promotes neurite outgrowth from cortical neurons grown on a monolayer of astrocytes	12.7538
10	Adipocyte enhancer-binding protein 1-like (<i>AEBP1</i>)	As a positive regulator of collagen fibrillogenesis, it is probably involved in the organization and remodeling of the extracellular matrix.	11.5426

The top 10 upregulated genes detected by SAM in the comparisons of the IA group with the sham group and the IA group with the RA group, with no genes upregulated in the comparison of the RA group with the sham group. A *Q* value ≤ 0.05 and $FC \geq 2$ or ≤ 0.5 were considered to indicate a significant change. Probes with no gene symbols were eliminated, and the differentially expressed genes were sorted by FC.

FC: fold change; IA: infarcted area; CNS: central nervous system; RA: remote area; SAM: significance analysis of microarray.

NR4A2 that were similar to that in the comparison of the IA group with the sham group. In addition, the gene expression of myosin light chain kinase family member 4 (*MYLK4*) and myosin light chain 7 (*MYL7*), which are involved in the cardiovascular system, was also downregulated in the comparison of the IA group with the RA group (Table 2).

Enriched pathways related to the differentially expressed genes in the ischemic heart

Pathway analysis was performed to detect the important signaling pathways associated with the pathological process

of prolonged myocardial ischemia, and the top 15 up- or downregulated pathways, sorted by *P* values, in the comparison of the IA group with the sham group are shown in Figure 2(A). No pathways were enriched in the comparison of the RA group with the sham group. Furthermore, the interactions between the enriched pathways were used to draw a pathway network to find the key pathways (Figure 2(B)). The results showed that in the comparison of the IA group with the sham group, pathways related to the extracellular matrix (ECM) exhibited the highest statistical significance among the upregulated pathways, including the ECM–receptor interaction and focal adhesion pathways

Table 2. Top 10 downregulated genes in hearts subjected to chronic myocardial ischemia.

ID	Gene name	Functions	FC
IA vs sham			
1	Corin, serine peptidase (<i>Corin</i>)	Serine-type endopeptidase involved in atrial natriuretic peptide (NPPA) and brain natriuretic peptide (NPPB) processing.	0.0829
2	Defensin beta 1 (<i>DEFB1</i>)	Has bactericidal activity. May act as a ligand for C-C chemokine receptor CCR6.	0.0863
3	NAD-dependent DNA ligase (<i>ligA</i>)	Located on the surface of the pathogenic leptospira and are reported as a potential virulent factor.	0.1193
4	Dehydrogenase/reductase SDR family member 7C-like (<i>DHRS7C</i>)	NADH-dependent oxidoreductase which catalyzes the oxidation of all-transretinol to all-transretinal. Plays a role in the regulation of cardiac and skeletal muscle metabolic functions.	0.1410
5	Phosphatidylethanolamine-binding protein 4 (<i>PEBP4</i>)	Promotes AKT phosphorylation, suggesting a possible role in the PI3K-AKT signaling pathway.	0.1641
6	Nuclear receptor subfamily 4 group A member 2 (<i>NR4A2</i>)	Transcriptional regulator which is important for the differentiation and maintenance of meso-diencephalic dopaminergic (mdDA) neurons during development.	0.1937
7	Flavin containing monooxygenase 2 (<i>FMO2</i>)	Catalyzes the oxidative metabolism of numerous xenobiotics, including mainly therapeutic drugs and insecticides that contain a soft nucleophile.	0.2242
8	TIMP metalloproteinase inhibitor 4 (<i>TIMP4</i>)	Complexes with metalloproteinases (such as collagenases) and irreversibly inactivates them by binding to their catalytic zinc cofactor.	0.2321
9	Amyotrophic lateral sclerosis 2 chromosome region candidate 12 (<i>ALS2CR12</i>)	Regulation of GTPase	0.2372
10	Fibroblast growth factor 12 (<i>FGF12</i>)	Involved in nervous system development and function. Involved in the positive regulation of voltage-gated sodium channel activity.	0.2475
RA vs sham			
1	Defensin beta 115 (<i>DEFB115</i>)	Has antibacterial activity	0.4717
IA vs RA			
1	Dehydrogenase/reductase SDR family member 7C-like (<i>DHRS7C</i>)	NADH-dependent oxidoreductase which catalyzes the oxidation of all-transretinol to all-transretinal. Plays a role in the regulation of cardiac and skeletal muscle metabolic functions.	0.0641
2	Defensin beta 1 (<i>DEFB1</i>)	Has bactericidal activity. May act as a ligand for C-C chemokine receptor CCR6.	0.0725
3	Interleukin 2 receptor, alpha (<i>IL2RA</i>)	Receptor for interleukin-2. The receptor is involved in the regulation of immune tolerance by controlling regulatory T-cells (TREGs) activity.	0.0962
4	Corin, serine peptidase (<i>Corin</i>)	Serine-type endopeptidase involved in atrial natriuretic peptide (NPPA) and brain natriuretic peptide (NPPB) processing.	0.1346
5	Myosin light chain kinase family, member 4 (<i>MYLK4</i>)	Have an important role in the development of colorectal cancer cells	0.1481
6	SPARC/osteonectin, cwcv and kazal like domains proteoglycan 3 (<i>SPOCK3</i>)	May participate in diverse steps of neurogenesis. Inhibits the processing of pro-matrix metalloproteinase 2 (MMP-2) by MT1-MMP and MT3-MMP. May interfere with tumor invasion.	0.2149
7	Glycerol-3-phosphate dehydrogenase 1 (<i>GPD1</i>)	Has glycerol-3-phosphate dehydrogenase activity.	0.2167
8	Fibroblast growth factor 12 (<i>FGF12</i>)	Involved in nervous system development and function. Involved in the positive regulation of voltage-gated sodium channel activity.	0.2219
9	Myosin light chain 7 (<i>MYL7</i>)	MYL7 is expressed in heart ventricles and atria, inactivation leads to embryonic lethality and abnormal cardiac morphogenesis.	0.2306
10	Nuclear receptor subfamily 4 group A member 2 (<i>NR4A2</i>)	Transcriptional regulator which is important for the differentiation and maintenance of meso-diencephalic dopaminergic (mdDA) neurons during development.	0.2450

The top 10 downregulated genes detected by SAM in the comparison of the IA group with the sham group, the IA group with the RA group, and the RA group with the sham group. A *Q* value ≤ 0.05 and $FC \geq 2$ or ≤ 0.5 were considered to indicate a significant change. Probes with no gene symbols were eliminated, and the differentially expressed genes were sorted by FC.

FC: fold change; IA: infarcted area; NAD: beta-Nicotinamide adenine dinucleotide trihydrate; NADH: Nicotinamide adenine dinucleotide; RA: remote area; SAM: significance analysis of microarray.

(Figure 2(A)), which also showed high degree values (numbers of pathways interacting with the pathway) of 7 and 11, respectively (Figure 2(B)). Furthermore, intracellular signaling pathways, including the PI3K-AKT signaling pathway with a degree of 8 and the TGF-beta signaling pathway with a degree of 6, and regulation of the actin cytoskeleton with a degree of 7 were also significantly upregulated by prolonged ischemia (Figure 2(A) and (B)). Among the downregulated pathways, the calcium signaling pathway showed the highest degree of 12, which may be closely related to the downregulation of cardiac muscle contraction after MI (Figure 2(A) and (B)).

GO analysis revealed the gene functions in three categories: biological process, molecular function, and cellular component. The enriched terms in the IA group compared

to the sham group showed that ECM interactions dominated the upregulated pathways in the late phase of MI, which was consistent with the results from pathway analysis. Moreover, among the terms of the biological process category associated with upregulated genes, a series of processes related to the developmental system were enriched, including the development of the skeletal system, heart, and cartilage (Figure 2(C)). In addition to the myocardial contraction pathways, which were also detected in pathway analysis, GO analysis also revealed other categories of terms that were associated with genes downregulated by prolonged ischemia, such as lipid metabolism, in which cellular lipid metabolic process, phospholipid biosynthetic process, phospholipid metabolic process, and fatty acid metabolic process were involved (Figure 2(C) and (E)).

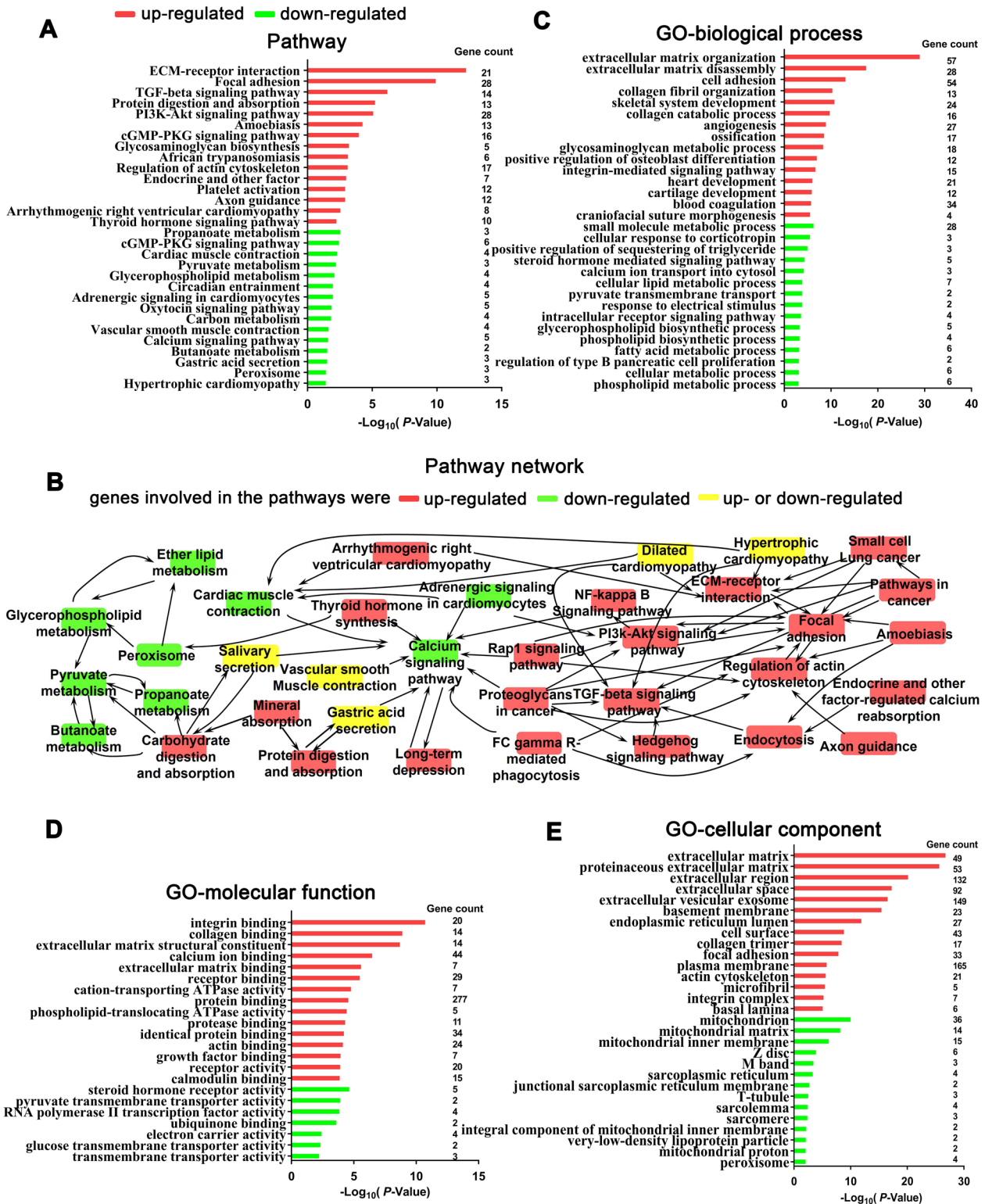


Figure 2. Significantly changed pathways or GO categories in the ischemic heart. (A) Pathway analysis of the up- or downregulated genes in the comparison of the IA and sham groups. (B) Pathway network analysis showed the interactions between the significantly changed pathways. Pathways involving all upregulated genes are colored red, those involving all downregulated genes are colored green, and those containing up- and downregulated genes are colored yellow. The arrow indicates the downstream direction in the pathway. GO analysis of the up- or downregulated terms in the (C) biological process, (D) molecular function, and (E) cellular component categories. In both pathway and GO analyses, the gene count showed the number of genes enriched for the corresponding terms. Significant changes were judged by a P value < 0.05 , and the terms were sorted by the $-\log_{10}(P\text{ value})$.

In addition, GO analysis also revealed enrichment in the category of mitochondrial components and function, which included the mitochondrial matrix and inner membrane,

the integral inner membrane component respiratory chain complex II, ubiquinone binding, and electron carrier activity (Figure 2(D) and 2(E)).

Discussion

Although the development of clinical reperfusion therapies for acute MI has greatly reduced the mortality resulting from MI, cardiac remodeling progressively occurs in the following months or years due to myocardial fibrosis in the IA and compensatory responses to ventricular dilatation in the non-IA, leading to a decreased ejection fraction and dysfunction of the heart.^{18–20} To further understand the molecular mechanisms during the late phase of cardiac remodeling, we employed DNA microarray technology to systematically explore the related genes and pathways involved in the development of cardiac remodeling on a genome-wide level. A rhesus monkey model of prolonged myocardial ischemia was established by LAD artery ligation. The IA and RA in the hearts from the MI group and the heart tissue from the sham group were collected at eight weeks after the surgery. We found that compared to the sham group, the IA group exhibited 941 upregulated transcripts and 380 downregulated transcripts, while the RA group exhibited only 8 downregulated transcripts. The significantly changed genes enriched in the present study, such as *NPPA/NPPB* and *corin*, and their related pathways, such as fibrosis-related pathways, cardioprotective pathways, and the cardiac systolic pathway, may act as key factors in regulating the development of heart remodeling.

We found multiple significantly changed biological processes involved in the IA, but few changes were found in the non-IA, as illustrated by the findings that 1321 and 8 transcripts were differentially expressed in the IA and RA groups compared to the sham group, respectively. The results were consistent with the histological examination results in our published studies, which showed that MI induced ventricular wall thinning, chamber dilatation, collagen deposition, and a capillary density decrease in the IA, with little or no damage found in RAs at eight weeks after MI in a monkey model.^{12,13}

Among the genes with significantly altered expression, *corin* encodes a serine protease promoting the hydrolysis of the inactive form pro-*NPPA* or pro-*NPPB* into the active form. The coordination of *corin* and *NPPA/NPPB* protein results in the prevention of heart failure during cardiac remodeling.^{21,22} However, disorder in mRNA expression was observed between *corin* (decreased) and *NPPA/NPPB* (increased) in the present study. The reduction in *corin* activation may lead to impairment of the cleavage function for natriuretic peptide.²³ Both *NPPA* and *corin* were ranked high in the significantly up- and downregulated gene lists, respectively, and *NPPB* expression was also dramatically increased, suggesting that the imbalance in the expression of *NPPA/NPPB* and *corin* may play a key role in aggravating cardiac dysfunction. In experimental dilated cardiomyopathy, the expression of *corin* mRNA is decreased during the pathological process, and this reduction starts before the development of heart failure, while the presence of *NPPA* and *NPPB* protein in plasma is only observed in the later stage of heart failure.²⁴ These observations suggest that *corin* may be valuable as a potential marker for the possibility of the development of heart failure after MI.

By GO/pathway analysis, we found several important pathways enriched in the late stage of MI. Among the upregulated pathways in the comparison of the IA group

with the sham group were ECM–receptor interaction and TGF- β signaling pathway, which may be the main feature in the chronic phase of MI given its highest statistical significance and high degree of association with other pathways. Excessive deposition of ECM-related proteins, mainly type I and type III collagen, contributes to the process of fibrosis and many other pathological remodeling processes after MI.^{25,26} The deposited collagen is produced by activated myofibroblasts, which are differentiated from fibroblasts. Phenotypic transformation is required for the regulation of TGF- β 1.^{27,28} Therapeutic strategies targeting the TGF- β signaling pathway improve left ventricular remodeling.^{29,30} The present study found that 21 and 14 differentially expressed genes were enriched in the ECM–receptor interaction and TGF- β signaling pathways, respectively, including genes encoding collagens that are involved in ECM–receptor interactions, such as *COL1A2*, *COL3A1*, *COL4A2*, *COL5A2*, *COL6A2*, and *COL6A3*. Reducing collagen deposition and promoting cardiomyocyte regeneration may be key strategies for heart remodeling therapy.

Furthermore, cardioprotective pathways were also found to be major features in hearts subjected to protracted ischemia, including focal adhesion and the PI3K-AKT signaling pathway, which all showed highly significant differences and high degrees. Focal adhesion contributes to interior and exterior cell signaling and to the connection of cells with the ECM, regulating cell motility,³¹ anchorage-dependent cell proliferation, and survival.³² Myocardial stress activates a cytoskeletal-based survival pathway, while inhibition of focal adhesion kinase abolishes ischemic preconditioning- or heat stress-induced PI3K-AKT signaling and its induced cardioprotection in ischemia/reperfusion injury.^{33,34} It shows the opposite effect in endothelial cells and cardiomyocytes; inhibition of PI3K β activity in endothelial cells protects the heart from heat failure, while PI3K β in cardiomyocytes protects against myocardial ischemic injury.³⁵ The present study found that 28 differentially expressed genes were enriched in focal adhesion or the PI3K-AKT signaling pathway, indicating that prolonged ischemia induced an extensive cardioprotective effect.

The most noteworthy pathway significantly downregulated by prolonged ischemia was the calcium signaling pathway, which was enriched for 5 differentially expressed genes and showed the highest degree of 12 among all enriched pathways. Ca²⁺, calmodulin, and Ca²⁺-dependent protein kinase II, which are involved in the calcium signaling pathway, regulate a series of proteins related to excitation–contraction coupling, and dysfunction of cell coupling leads to arrhythmias.³⁶ Targeting the calcium signaling pathway has been applied to the treatment of arrhythmias in heart failure,³⁷ and the loss of myocardial contraction-related genes may be an important point of concern.

In addition to the rhesus monkey model, several small animals, such as mice and rats, and large animals, such as dogs and pigs, have been widely used in IHD-related studies.^{38–40} Among those transcriptomic studies, in the rat MI model (at least eight weeks after MI), the main upregulated pathways were cytoskeletal and ECM proteins. Gene expression levels of *NPPA*, *NPPB*, *collagen III*, *biglycan*, *fibronectin*, *biglycan*, *THBS4*, *lysyl oxidase*, and *complement factor B* were significantly upregulated, and contractile genes

were downregulated.^{41–43} These changes were consistent with our study. While several changes, including the matrix-related gene *osteopontin*, returned to baseline between two and six weeks after surgery,⁴¹ the appearance of upregulated genes (*atrial natriuretic factor* and ECM genes) in the interventricular septum⁴² differed from our study, with continuously elevated expression levels of *osteopontin* and undetectable upregulated genes in the RA group in our monkey model. Compared with a study using a chronic ischemic swine model of MI, our results presented similar changes in hypertrophic cardiomyopathy, cardiogenesis, and embryonic stem cell pluripotency and varying degrees of apoptosis signaling and hypoxia signaling.⁴⁴

In ischemia and reperfusion (I/R) injury, another cause of MI, several remarkably changed pathways were also observed by transcriptome analysis. Bile acid pathway derivatives and intermediates predominated in the late reperfusion phases in an I/R porcine model.⁴⁵ Antigen immunomodulatory pathways were activated and neprilysin was downregulated in both ischemia-affected and non-affected zones during the late phase of cardio protection in a domestic pig model.⁴⁶ A study using a rat model of I/R showed that apoptosis is important in the pathogenesis of MI, and ECM proteins such as types I and III collagen were upregulated in late inflammatory phases.⁴⁷ The changes in ECM genes were also prominent in our study.

Experimental animal models of MI that can mimic human pathophysiology are essential for the translation study of clinical applications. Some disadvantages exist in small animal models, such as the smaller size of the heart, the differences in anatomy and physiology of the coronary arteries, the faster contractile kinetics, and the different sensitivity to exercise and anesthetics compared with those of humans.^{48,49} It was found that in a rat MI model, although similar changes in mitogenic cardiomyocytes that were present in humans were observed, they were spatially and temporally restricted. Using a large animal model to perform multicenter validation is the final step of validation prior to clinical testing.⁵⁰ Taking this into consideration, a non-human primate MI model of monkeys was employed in the present study because monkeys are more similar to humans in terms of heart size, coronary anatomy, and physiology, and are encouraged to be used as an animal model in preclinical studies.^{49,51,52}

In conclusion, the present study employed an MI model of rhesus monkeys to identify the key genes and pathways involved in promoting the development of pathological myocardial remodeling during chronic ischemia. Asynchrony in the expression of *corin* and *NPPA/NPPB* may aggravate cardiac remodeling. Moreover, ECM–receptor interactions, the TGF- β signaling pathway, focal adhesion, the PI3K-AKT signaling pathway, and the calcium signaling pathway may be critical for the development of pathological myocardial remodeling. Further studies will focus on the mechanisms of heart failure caused by the loss of coordination between the significantly changed pathways.

AUTHORS' CONTRIBUTIONS

WZ and YJK conceived and coordinated the research. XL arranged most of the DNA microarray data analysis, JZ extracted the total RNA and did the RT-qPCR analysis, PL provided help

to the data analysis, PH conducted the animal model construction, WZ and XL wrote the manuscript, and YJK edited the manuscript. All authors participated in the design, interpretation of the results, and review of the manuscript.

ACKNOWLEDGEMENTS

The authors thank CapitalBio Corporation Company, Beijing, China, and Mr Bingqiang Ding for technical support.

DECLARATION OF CONFLICTING INTERESTS

The author(s) declared no potential conflicts of interest with respect to the research, authorship, and/or publication of this article.

FUNDING

The author(s) disclosed receipt of the following financial support for the research, authorship, and/or publication of this article: This work was supported by National Natural Science Foundation of China (grant number 81600214) and Yunnan Province Basic Research Program Youth Project (grant number 202001AU070143).

ORCID ID

Wenjing Zhang  <https://orcid.org/0000-0002-6694-6072>

REFERENCES

- Arnett DK, Blumenthal RS, Albert MA, Buroker AB, Goldberger ZD, Hahn EJ, Himmelfarb CD, Khera A, Lloyd-Jones D, McEvoy JW, Michos ED, Miedema MD, Munoz D, Smith SC Jr, Virani SS, Williams KA Sr, Yeboah J, Ziaeian B. 2019 ACC/AHA guideline on the primary prevention of cardiovascular disease: executive summary: a report of the American College of Cardiology/American Heart Association Task Force on clinical practice guidelines. *J Am Coll Cardiol* 2019;**74**:1376–414
- Lopez AD, Mathers CD. Measuring the global burden of disease and epidemiological transitions: 2002-2030. *Ann Trop Med Parasitol* 2006;**100**:481–99
- Ding HS, Yang J, Chen P, Yang J, Bo SQ, Ding JW, Yu QQ. The HMGB1-TLR4 axis contributes to myocardial ischemia/reperfusion injury via regulation of cardiomyocyte apoptosis. *Gene* 2013;**527**:389–93
- Kitahara T, Takeishi Y, Harada M, Niizeki T, Suzuki S, Sasaki T, Ishino M, Bilim O, Nakajima O, Kubota I. High-mobility group box 1 restores cardiac function after myocardial infarction in transgenic mice. *Cardiovasc Res* 2008;**80**:40–6
- Gaudron P, Eilles C, Kugler I, Ertl G. Progressive left ventricular dysfunction and remodeling after myocardial infarction. Potential mechanisms and early predictors. *Circulation* 1993;**87**:755–63
- White HD, Norris RM, Brown MA, Brandt PW, Whitlock RM, Wild CJ. Left-ventricular end-systolic volume as the major determinant of survival after recovery from myocardial-infarction. *Circulation* 1987;**76**:44–51
- Yi W, Zhu R, Hou X, Wu F, Feng R. Integrated analysis reveals S100a8/a9 regulates autophagy and apoptosis through the MAPK and PI3K-AKT signaling pathway in the early stage of myocardial infarction. *Cells* 2022;**11**:1911
- Han Y, Duan B, Wu J, Zheng Y, Gu Y, Cai X, Lu C, Wu X, Li Y, Gu X. Analysis of time series gene expression and DNA methylation reveals the molecular features of myocardial infarction progression. *Front Cardiovasc Med* 2022;**9**:912454
- Olivetti G, Capasso JM, Meggs LG, Sonnenblick EH, Anversa P. Cellular basis of chronic ventricular remodeling after myocardial infarction in rats. *Circ Res* 1991;**68**:856–69
- Weber KT, Sun Y, Tyagi SC, Cleutjens JP. Collagen network of the myocardium: function, structural remodeling and regulatory mechanisms. *J Mol Cell Cardiol* 1994;**26**:279–92

11. Moslehi J, Minamishima YA, Shi J, Neuberger D, Charytan DM, Padera RF, Signoretti S, Liao R, Kaelin WG Jr. Loss of hypoxia-inducible factor prolyl hydroxylase activity in cardiomyocytes phenocopies ischemic cardiomyopathy. *Circulation* 2010;**122**:1004–16
12. Zhang W, Zhao X, Xiao Y, Chen J, Han P, Zhang J, Fu H, James Kang Y. The association of depressed angiogenic factors with reduced capillary density in the Rhesus monkey model of myocardial ischemia. *Metallomics* 2016;**8**:654–62
13. Xiao Y, Nie X, Han P, Fu H, James Kang Y. Decreased copper concentrations but increased lysyl oxidase activity in ischemic hearts of rhesus monkeys. *Metallomics* 2016;**8**:973–80
14. Duggan DJ, Bittner M, Chen Y, Meltzer P, Trent JM. Expression profiling using cDNA microarrays. *Nat Genet* 1999;**21**:10–4
15. Irizarry RA, Hobbs B, Collin F, Beazer-Barclay YD, Antonellis KJ, Scherf U, Speed TP. Exploration, normalization, and summaries of high density oligonucleotide array probe level data. *Biostatistics* 2003;**4**:249–64
16. Chen HH, Burnett JC Jr. The natriuretic peptides in heart failure: diagnostic and therapeutic potentials. *Proc Assoc Am Physicians* 1999;**111**:406–16
17. Yan W, Wu F, Morser J, Wu Q. Corin, a transmembrane cardiac serine protease, acts as a pro-atrial natriuretic peptide-converting enzyme. *Proc Natl Acad Sci U S A* 2000;**97**:8525–9
18. Kostuk WJ, Kazamias TM, Gander MP, Simon AL, Ross J Jr. Left ventricular size after acute myocardial infarction. Serial changes and their prognostic significance. *Circulation* 1973;**47**:1174–9
19. Eaton LW, Weiss JL, Bulkley BH, Garrison JB, Weisfeldt ML. Regional cardiac dilatation after acute myocardial infarction: recognition by two-dimensional echocardiography. *N Engl J Med* 1979;**300**:57–62
20. Reimer KA, Lowe JE, Rasmussen MM, Jennings RB. The wavefront phenomenon of ischemic cell death. 1. Myocardial infarct size vs duration of coronary occlusion in dogs. *Circulation* 1977;**56**:786–94
21. Tripathi R, Sullivan R, Fan TM, Wang D, Sun Y, Reed GL, Gladysheva IP. Enhanced heart failure, mortality and renin activation in female mice with experimental dilated cardiomyopathy. *PLoS ONE* 2017;**12**:e0189315
22. Niu Y, Zhang S, Gu X, Zhou T, Li F, Liu M, Wu Q, Dong N. Recombinant soluble corin improves cardiac function in mouse models of heart failure. *J Am Heart Assoc* 2021;**10**:e0119961
23. Chen S, Sen S, Young D, Wang W, Moravec CS, Wu Q. Protease corin expression and activity in failing hearts. *Am J Physiol Heart Circ Physiol* 2010;**299**:H1687–92
24. Tripathi R, Wang D, Sullivan R, Fan TH, Gladysheva IP, Reed GL. Depressed corin levels indicate early systolic dysfunction before increases of atrial natriuretic peptide/B-type natriuretic peptide and heart failure development. *Hypertension* 2016;**67**:362–7
25. MacKenna D, Summerour SR, Villarreal FJ. Role of mechanical factors in modulating cardiac fibroblast function and extracellular matrix synthesis. *Cardiovasc Res* 2000;**46**:257–63
26. Hong D, Zeng X, Xu W, Ma J, Tong Y, Chen Y. Altered profiles of gene expression in curcumin-treated rats with experimentally induced myocardial infarction. *Pharmacol Res* 2010;**61**:142–8
27. Ma Y, de Castro Bras LE, Toba H, Iyer RP, Hall ME, Winniford MD, Lange RA, Tyagi SC, Lindsey ML. Myofibroblasts and the extracellular matrix network in post-myocardial infarction cardiac remodeling. *Pflugers Arch* 2014;**466**:1113–27
28. Desmouliere A, Geinoz A, Gabbiani F, Gabbiani G. Transforming growth factor-beta 1 induces alpha-smooth muscle actin expression in granulation tissue myofibroblasts and in quiescent and growing cultured fibroblasts. *J Cell Biol* 1993;**122**:103–11
29. Han A, Lu Y, Zheng Q, Zhang J, Zhao Y, Zhao M, Cui X. Qiliqiangxin attenuates cardiac remodeling via inhibition of TGF-beta1/Smad3 and NF-kappaB signaling pathways in a rat model of myocardial infarction. *Cell Physiol Biochem* 2018;**45**:1797–806
30. Okada H, Takemura G, Kosai K, Li Y, Takahashi T, Esaki M, Yuge K, Miyata S, Maruyama R, Mikami A, Minatoguchi S, Fujiwara T, Fujiwara H. Postinfarction gene therapy against transforming growth factor-beta signal modulates infarct tissue dynamics and attenuates left ventricular remodeling and heart failure. *Circulation* 2005;**111**:2430–7
31. Hauck CR, Hsia DA, Ilic D, Schlaepfer DD. v-Src SH3-enhanced interaction with focal adhesion kinase at beta 1 integrin-containing invadopodia promotes cell invasion. *J Biol Chem* 2002;**277**:12487–90
32. Miranti CK, Brugge JS. Sensing the environment: a historical perspective on integrin signal transduction. *Nat Cell Biol* 2002;**4**:E83–90
33. Perricone AJ, Bivona BJ, Jackson FR, Vander Heide RS. Conditional knockout of myocyte focal adhesion kinase abrogates ischemic preconditioning in adult murine hearts. *J Am Heart Assoc* 2013;**2**:e000457
34. Wei H, Vander Heide RS. Ischemic preconditioning and heat shock activate Akt via a focal adhesion kinase-mediated pathway in Langendorff-perfused adult rat hearts. *Am J Physiol Heart Circ Physiol* 2010;**298**:H152–7
35. Chen X, Zhabeyev P, Azad AK, Wang W, Minerath RA, DesAulniers J, Grueter CE, Murray AG, Kassiri Z, Vanhaesebroeck B, Oudit GY. Endothelial and cardiomyocyte PI3Kbeta divergently regulate cardiac remodeling in response to ischemic injury. *Cardiovasc Res* 2019;**115**:1343–56
36. Sanchez JA, Rodriguez-Sinovas A, Fernandez-Sanz C, Ruiz-Meana M, Garcia-Dorado D. Effects of a reduction in the number of gap junction channels or in their conductance on ischemia-reperfusion arrhythmias in isolated mouse hearts. *Am J Physiol Heart Circ Physiol* 2011;**301**:H2442–53
37. Rokita AG, Anderson ME. New therapeutic targets in cardiology: arrhythmias and Ca2+ /calmodulin-dependent kinase II (CaMKII). *Circulation* 2012;**126**:2125–39
38. Zhong Y, Yu X, Li X, Zhou H, Wang Y. Augmented early aged neutrophil infiltration contributes to late remodeling post myocardial infarction. *Microvasc Res* 2022;**139**:104268
39. Docshin PM, Karpov AA, Mametov MV, Ivkin DY, Kostareva AA, Malashicheva AB. Mechanisms of regenerative potential activation in cardiac mesenchymal cells. *Biomedicines* 2022;**10**:1283
40. Monguio-Tortajada M, Prat-Vidal C, Martinez-Falguera D, Teis A, Soler-Botija C, Courageux Y, Munizaga-Larroude M, Moron-Font M, Bayes-Genis A, Borrás FE, Roura S, Galvez-Monton C. Acellular cardiac scaffolds enriched with MSC-derived extracellular vesicles limit ventricular remodeling and exert local and systemic immunomodulation in a myocardial infarction porcine model. *Theranostics* 2022;**12**:4656–70
41. Sehl PD, Tai JT, Hillan KJ, Brown LA, Goddard A, Yang R, Jin H, Lowe DG. Application of cDNA microarrays in determining molecular phenotype in cardiac growth, development, and response to injury. *Circulation* 2000;**101**:1990–9
42. Stanton LW, Garrard LJ, Damm D, Garrick BL, Lam A, Kapoun AM, Zheng Q, Protter AA, Schreiner GF, White RT. Altered patterns of gene expression in response to myocardial infarction. *Circ Res* 2000;**86**:939–45
43. Jin H, Yang R, Awad TA, Wang F, Li W, Williams SP, Ogasawara A, Shimada B, Williams PM, de Feo G, Paoni NF. Effects of early angiotensin-converting enzyme inhibition on cardiac gene expression after acute myocardial infarction. *Circulation* 2001;**103**:736–42
44. Prat-Vidal C, Galvez-Monton C, Nonell L, Puigdecenet E, Astier L, Sole F, Bayes-Genis A. Identification of temporal and region-specific myocardial gene expression patterns in response to infarction in swine. *PLoS ONE* 2013;**8**:e54785
45. Goetzman E, Gong Z, Rajasundaram D, Muzumdar I, Goodchild T, Lefer D, Muzumdar R. Serum metabolomics reveals distinct profiles during ischemia and reperfusion in a porcine model of myocardial ischemia-reperfusion. *Int J Mol Sci* 2022;**23**:6711
46. Pavo N, Lukovic D, Zlabinger K, Zimba A, Lorant D, Goliasch G, Winkler J, Pils D, Auer K, Jan Ankersmit H, Giricz Z, Baranyai T, Sarkozy M, Jakab A, Garamvolgyi R, Emmert MY, Hoerstrup SP, Hausenloy DJ, Ferdinandy P, Maurer G, Gyongyosi M. Sequential activation of different pathway networks in ischemia-affected and non-affected myocardium, inducing intrinsic remote conditioning to prevent left ventricular remodeling. *Sci Rep* 2017;**7**:43958
47. Roy S, Khanna S, Kuhn DE, Rink C, Williams WT, Zweier JL, Sen CK. Transcriptome analysis of the ischemia-reperfusion remodeling

- myocardium: temporal changes in inflammation and extracellular matrix. *Physiol Genomics* 2006;**25**:364–74
48. Ciszek B, Skubiszewska D, Ratajska A. The anatomy of the cardiac veins in mice. *J Anat* 2007;**211**:53–63
49. Seok J, Warren HS, Cuenca AG, Mindrinos MN, Baker HV, Xu W, Richards DR, McDonald-Smith GP, Gao H, Hennessy L, Finnerty CC, Lopez CM, Honari S, Moore EE, Minei JP, Cuschieri J, Bankey PE, Johnson JL, Sperry J, Nathens AB, Billiar TR, West MA, Jeschke MG, Klein MB, Gamelli RL, Gibran NS, Brownstein BH, Miller-Graziano C, Calvano SE, Mason PH, Cobb JP, Rahme LG, Lowry SF, Maier RV, Moldawer LL, Herndon DN, Davis RW, Xiao W, Tompkins RG, Inflammation and Host Response to Injury, Large Scale Collaborative Research Program. Genomic responses in mouse models poorly mimic human inflammatory diseases. *Proc Natl Acad Sci U S A* 2013;**110**:3507–12
50. Lecour S, Andreadou I, Botker HE, Davidson SM, Heusch G, Ruiz-Meana M, Schulz R, Zuurbier CJ, Ferdinandy P, Hausenloy DJ, on behalf of the European Union CCAC. IMproving Preclinical Assessment of Cardioprotective Therapies (IMPACT) criteria: guidelines of the EU-CARDIOPROTECTION COST action. *Basic Res Cardiol* 2021;**116**:52
51. Tohno Y, Tohno S, Laleva L, Ongkana N, Minami T, Satoh H, Oishi T, Hayashi M, Sinthubua A, Suwannahoy P, Mahakkanukrauh P. Age-related changes of elements in the coronary arteries of monkeys in comparison with those of humans. *Biol Trace Elem Res* 2008;**125**:141–53
52. Clarkson TB, Prichard RW, Morgan TM, Petrick GS, Klein KP. Remodeling of coronary arteries in human and nonhuman primates. *JAMA* 1994;**271**:289–94

(Received September 5, 2022, Accepted December 20, 2022)